To appear in Proc. of Snowbird TeV Gamma-Ray Workshop
ed. B. L. Dingus (AIP, New York, 1999)

Modelling Hard Gamma-Ray Emission From Supernova Remnants

Matthew G. Baring†

Laboratory for High Energy Astrophysics, Code 661
NASA Goddard Space Flight Center, Greenbelt, MD 20771
baring@lheavx.gsfc.nasa.gov
† *Universities Space Research Association*

Abstract. The observation by the CANGAROO experiment of TeV emission from SN 1006, in conjunction with several instances of non-thermal X-ray emission from supernova remnants, has led to inferences of super-TeV electrons in these extended sources. While this is sufficient to propel the theoretical community in their modelling of particle acceleration and associated radiation, the anticipated emergence in the next decade of a number of new experiments probing the TeV and sub-TeV bands provides further substantial motivation for modellers. In particular, the quest for obtaining unambiguous gamma-ray signatures of cosmic ray ion acceleration defines a "Holy Grail" for observers and theorists alike. This review summarizes theoretical developments in the prediction of MeV–TeV gamma-rays from supernova remnants over the last five years, focusing on how global properties of models can impact, and be impacted by, hard gamma-ray observational programs, thereby probing the supernova remnant environment. Properties of central consideration include the maximum energy of accelerated particles, the density of the unshocked interstellar medium, the ambient magnetic field, and the relativistic electron-to-proton ratio. Criteria for determining good candidate remnants for observability in the TeV band are identified.

INTRODUCTION

It is widely believed that supernova remnants (SNRs) are the primary sources of cosmic-ray ions and electrons up to energies of at least $\sim 10^{15}$ eV, where the so-called *knee* in the spectrum marks a deviation from almost pure power-law behavior. Such cosmic rays are presumed to be generated by diffusive (also called first-order Fermi) acceleration at the remnants' forward shocks. These cosmic rays can generate gamma rays via interactions with the ambient interstellar medium, including nuclear interactions between relativistic and cold interstellar ions, by bremsstrahlung of energetic electrons colliding with the ambient gas, and inverse Compton (IC) emission off cosmic background radiation. Rudimentary models of gamma-ray production in remnants involving nuclear interactions date back to the late 1970s [1,2]. These preceded the first tentative associations of two COS-B

gamma-ray sources [3] with the remnants γ Cygni and W28. Apart from the work of Dorfi [4], who provided the first model including a more sophisticated study of non-linear effects of shock acceleration to treat gamma-ray production, the study of gamma-ray SNRs remained quietly in the background until the observational program of the EGRET experiment aboard the Compton Gamma Ray Observatory. This provided a large number of unidentified sources above 50 MeV, a handful of which have interesting associations with relatively young SNRs [5].

Following the EGRET advances, the modelling of gamma-ray and other non-thermal emission from supernova remnants "burgeoned," beginning with the paper of Drury, Aharonian, & Völk [6] (hereafter DAV94), who computed the photon spectra expected from the decay of neutral pions generated in collisions of power-law shock-accelerated ions with those of the interstellar medium (ISM). This work spawned a number of subsequent papers that used different approaches, as discussed in the next section, and propelled the TeV gamma-ray astronomy community into a significant observational program given the prediction of substantial TeV fluxes from the DAV94 model. The initial expectations of TeV gamma-ray astronomers were dampened by the lack of success of the Whipple and HEGRA groups [7–9] in detecting emission from SNRs after a concerted campaign. While sectors of the community contended that the constraining TeV upper limits posed difficulties for SNR shock acceleration models, these observational results were naturally explained [10–12] by the maximum particle energies expected (in the 1–50 TeV range) in remnants and the concomitant anti-correlation between maximum energy of gamma-ray emission and the gamma-ray luminosity [13] (discussed below).

The observational breakthrough in this field came with the recent report of a spatially-resolved detection of SN1006 (not accessible by northern hemisphere atmospheric Čerenkov telescopes (ACTs) such as Whipple and HEGRA) by the CANGAROO experiment [14] at energies above 1.7 TeV. The interpretation (actually predicted for SN 1006 by [10,15]) that evolved was that this emission was due to energetic electrons accelerated in the low density environs of this high-latitude remnant, generating flat-spectrum inverse Compton radiation seeded by the cosmic microwave background. This suggestion was influenced, if not motivated by the earlier detection [16] of the steep non-thermal X-ray emission from SN 1006 that has been assumed to be the upper end of a broad synchrotron component, implying the presence of electrons in the 20–100 TeV range. Studies of gamma-ray emission from remnants have adapted to this discovery by suggesting (e.g. [11,13]) that galactic plane remnants such as Cas A that possess denser interstellar surroundings may have acceleration and emission properties distinct from high-latitude sources; the exploration of such a contention may be on the horizon, given the detection of Cas A by HEGRA announced at this meeting [17]. Given the complexity of recent shock acceleration/SNR emission models, the range of spectral possibilities is considerable, and a source of confusion for both theorists and observers. It is the aim of this paper to elucidate the study of gamma-ray remnants by pinpointing the key spectral variations/trends with changes in model parameters, and thereby identify the principal parameters that impact TeV astronomy programs.

MODELS: A BRIEF HISTORY

Reviews of recent models of gamma-ray emission from SNRs can be found in [11,13,18,19]; a brief exposition is given here. Drury, Aharonian, & Völk [6] provided impetus for recent developments when they calculated gamma-ray emission from protons using the time-dependent, two-fluid analysis (thermal ions plus cosmic rays) of [20], following on from the similar work of [4]. They assumed a power-law proton spectrum, so that no self-consistent determination of spectral curvature to the distributions [21–23] or temporal or spatial limits to the maximum energy of acceleration was made. The omission of environmentally-determined high energy cutoffs in their model was a critical driver for the interpretative discussion that ensued. [6] found that during much of Sedov evolution, maximal diffusion length scales are considerably less than a remnant's shock radius.

Gaisser, et al. [24] computed emission from bremsstrahlung, inverse Compton scattering, and pion-decay from proton interactions, but did not consider non-linear shock dynamics or time-dependence and assumed test-particle power-law distributions of protons and electrons with arbitrary e/p ratios. In order to suppress the flat inverse Compton component and thereby accommodate the EGRET observations of γ Cygni and IC443, [24] obtained approximate constraints on the ambient matter density and the primary e/p ratio.

A time-dependent model of gamma-ray emission from SNRs using the Sedov solution for the expansion was presented by Sturner, et al. [12]. They numerically solved equations for electron and proton distributions subject to cooling by inverse Compton scattering, bremsstrahlung, π^0 decay, and synchrotron radiation (to supply a radio flux). Expansion dynamics and non-linear acceleration effects were not treated, and power-law spectra were assumed. Sturner et al. (1997) introduced cutoffs in the distributions of the accelerated particles (following [10,25,26]), which are defined by the limits (discussed below) on the achievable energies in Fermi acceleration. Hence, given suitable model parameters, they were able to accommodate the constraints imposed by Whipple's upper limits [9] to γ Cygni and IC 443.

To date, the two most complete models coupling the time-dependent dynamics of the SNR to cosmic ray acceleration are those of Berezhko & Völk [27], based on the model of [28], and Baring et al. [13]. Berezhko & Völk numerically solve the gas dynamic equations including the cosmic ray pressure and Alfvén wave dissipation, following the evolution of a spherical remnant in a homogeneous medium. Originally only pion decay was considered, though this has now been extended [32] to include other components. Baring et al. simulate the diffusion of particles in the environs of steady-state planar shocks via a well-documented Monte Carlo technique [23,29] that has had considerable success in modelling particle acceleration at the Earth bow shock [30] and interplanetary shocks [31] in the heliosphere. They also solve the gas dynamics numerically, and incorporate the principal effects of time-dependence through constraints imposed by the Sedov solution.

These two refined models possess a number of similarities. Both generate upward spectral curvature (predicted by [21]; see the review in [11]), a signature that is a

consequence of the higher energy particles diffusing on larger scales and therefore sampling larger effective compressions, and both obtain overall compression ratios r well above standard test-particle Rankine-Hugoniot values. Yet, there are two major differences between these two approaches. First Berezhko et al. [27,32] include time-dependent details of energy dilution near the maximum particle energy self-consistently, while Baring et al. [13] mimic this property by using the Sedov solution to constrain parametrically the maximum scale of diffusion (defining an escape energy). These two approaches merge in the Sedov phase [33], because particle escape from strong shocks is a fundamental part of the non-linear acceleration process and is determined primarily by energy and momentum conservation, not time-dependence or a particular geometry. Second, [13] injects ions into the non-linear acceleration process automatically from the thermal population, and so determine the dynamical feedback self-consistently, whereas [27] must specify the injection efficiency as a free parameter. Berezhko & Ellison [33] recently demonstrated that, for most cases of interest, the shock dynamics are relatively insensitive to the efficiency of injection, and that there is good agreement between the two approaches when the Monte Carlo simulation [13,29] specifies injection for the model of [27]. This convergence of results from two complimentary methods is reassuring to astronomers, and underpins the expected reliability of emission models to the point that a hybrid "simple model" has been developed [34] to describe the essential acceleration features of both techniques. This has been extended to a new and comprehensive parameter survey [35] of broad-band SNR emission that provides results that form the basis of much of the discussion below.

GLOBAL THEORETICAL PREDICTIONS

Since there is considerable agreement between the most developed acceleration/emission models, we are in the comfortable position of being able to identify the salient global properties that should be characteristics of any particular model. Clearly a treatment of non-linear dynamics and associated spectral curvature are an essential ingredient to more accurate predictions of emission fluxes, particularly in the X-ray and gamma-ray bands where large dynamic ranges in particle momenta are sampled, so that discrepancies of factors of a few or more arise when test-particle power-laws are used. Concomitantly, test-particle shock solutions considerably over-estimate [29,34,35] the dissipational heating of the downstream plasma in high Mach number shocks, thereby introducing errors that propagate into predictions of X-ray emission and substantially influence the overall normalization of hard X-ray to gamma-ray emission (which depends on the plasma temperature [13,35]). These points emphasize that a cohesive treatment of the entire particle distributions is requisite for the accuracy of a given model.

In addition, finite maximum energies of cosmic rays imposed by spatial and temporal acceleration constraints (e.g. [13,36]) must be integral to any model, influencing feedback that modifies the non-linear acceleration problem profoundly.

In SNR evolutionary scenarios, a natural scaling of this maximum energy $E_{\rm max}$ arises, defined approximately by the energy attained at the onset of the Sedov phase [13,36]:

$$E_{\rm max} \sim 60 \frac{Q}{\eta} \left(\frac{B_{\rm ISM}}{3\mu{\rm G}}\right) \left(\frac{n_{\rm ISM}}{1\,{\rm cm}^{-3}}\right)^{-1/3} \left(\frac{\mathcal{E}_{\rm SN}}{10^{51}{\rm erg}}\right)^{1/2} \left(\frac{M_{\rm ej}}{M_\odot}\right)^{-1/6} {\rm TeV} \ , \qquad (1)$$

where Q is the particle's charge, η (≥ 1) is the ratio between its scattering mean-free-path and its gyroradius, $\mathcal{E}_{\rm SN}$ is the supernova energy, $M_{\rm ej}$ is its ejecta mass, and other quantities are self-explanatory. At earlier epochs, the maximum energy scales approximately linearly with time, while in the Sedov phase, it slowly asymptotes [13,37] to a value a factor of a few above that in Eq. (1).

Three properties emerge as global signatures of models that impact observational programs. The first is that there is a strong anti-correlation of $E_{\rm max}$ (and therefore the maximum energy of gamma-ray emission) with gamma-ray luminosity, first highlighted by [13]. High ISM densities are conducive to brighter sources in the EGRET to sub-TeV band [13,27,35], but reduce $E_{\rm max}$ in Eq. (1) and accordingly act to inhibit detection by ACTs. Low ISM magnetic fields produce a similar trend, raising the gamma-ray flux by flattening the cosmic ray distribution (discussed below). Clearly, high density, low $B_{\rm ISM}$ remnants are the best candidates for producing cosmic rays up to the knee. Fig. 1 displays a sample model spectrum for Cas A, which has a high density, high $B_{\rm ISM}$ environment. In it the various spectral components are evident, and the lower $E_{\rm max}$ for electrons (relative to that for protons) that is generated by strong cooling is evident in the bremsstrahlung and inverse Compton spectra.

The other two global properties are of a temporal nature. The first is the approximate constancy of the observed gamma-ray flux (and $E_{\rm max}$ [37]) in time during Sedov phase, an insensitivity first predicted by [4] and confirmed in the analyses of [6,13,37]. The origin of this insensitivity to SNR age $t_{\rm SNR}$ is an approximate compensation between the SNR volume $\mathcal{V}$ that scales as $t_{\rm SNR}^{6/5}$ (radius $\propto t_{\rm SNR}^{2/5}$) in the Sedov phase, and the normalization coefficient $\mathcal{N}$ of the roughly E^{-2} particle distribution function: since the shock speed (and therefore also the downstream plasma temperature $T_{\rm pd}$) declines as $t_{\rm SNR}^{-3/5}$, it follows that $\mathcal{N} \propto T_{\rm pd}^2 \propto t_{\rm SNR}^{-6/5}$ and flux $\propto \mathcal{N}\mathcal{V} \approx$ const. There is also a limb brightening with age [6] that follows from the constant maximum particle length scale concurrent with continuing expansion.

Key Parameters and Model Behavioural Trends

The principal aim here is to distill the complexity of non-linear acceleration models for time-dependent SNR expansions and discern the key parameters controlling spectral behaviour and simple reasons for behavioural trends. This should elucidate for theorist and experimentalist alike the scientific gains to be made by present and next generation experimental programs. Parameters are grouped according to them

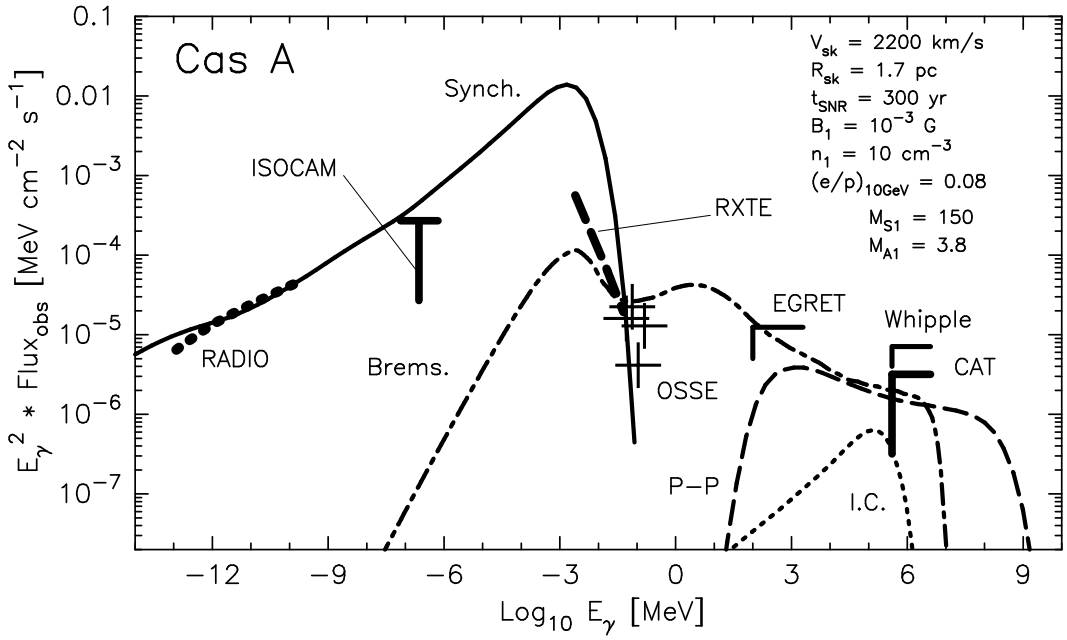

FIGURE 1. The Cassiopeia A spectrum from the Monte Carlo acceleration calculation of Ellison et al. ([38], see this for detailed referencing of the data sources). The model photons come from a single set of proton, helium, and electron spectra calculated with the upstream parameters shown in the figure. A single normalization factor has been applied to all components to match the radio flux. Note that the bremsstrahlung and inverse Compton (IC) emission cuts off at a much lower energy than the pion decay radiation due to the synchrotron losses the electrons experience. In these results, the IC component does not include a synchrotron self-Compton contribution.

being of model origin and environmental nature (trends associated with the age of a remnant were discussed just above), and details can be found in the comprehensive survey of Ellison, Berezhko & Baring [35].

There are three relevant *model* parameters in non-linear acceleration, the ratio of downstream electron and proton temperatures $T_{\rm ed}/T_{\rm pd}$, the injection efficiency $\eta_{\rm inj}$ (after [27,28]), and the electron-to-proton ratio $(e/p)_{\rm rel}$ at relativistic energies (i.e. $\gtrsim 1-10\,$GeV). The injection efficiency is the most crucial of these, since it controls the pressure contained in non-thermal ions, and therefore the non-linearity of the acceleration process. It mainly impacts the X-ray to soft gamma-ray bremsstrahlung contribution, a component that is generally dominated by pion decay emission in the hard gamma-ray band. The shape and normalization of the π^0 decay gamma-rays is only affected when $\eta_{\rm inj}$ drops below 10^{-4} and the shock solution becomes close to the test-particle one, i.e. an overall spectral steepening arises. Variations in $(e/p)_{\rm rel}$ influence the strength of the inverse Compton and bremsstrahlung components, which modify the total gamma-ray flux only if $(e/p)_{\rm rel} \gtrsim 0.1$, a high value relative to cosmic ray abundances, or the ambient field is strong.

The most interesting behavioural trends are elicited by the *environmental* parameters $n_{\rm ISM}$ and $B_{\rm ISM}$, and the results adapted from [35] are illustrated in

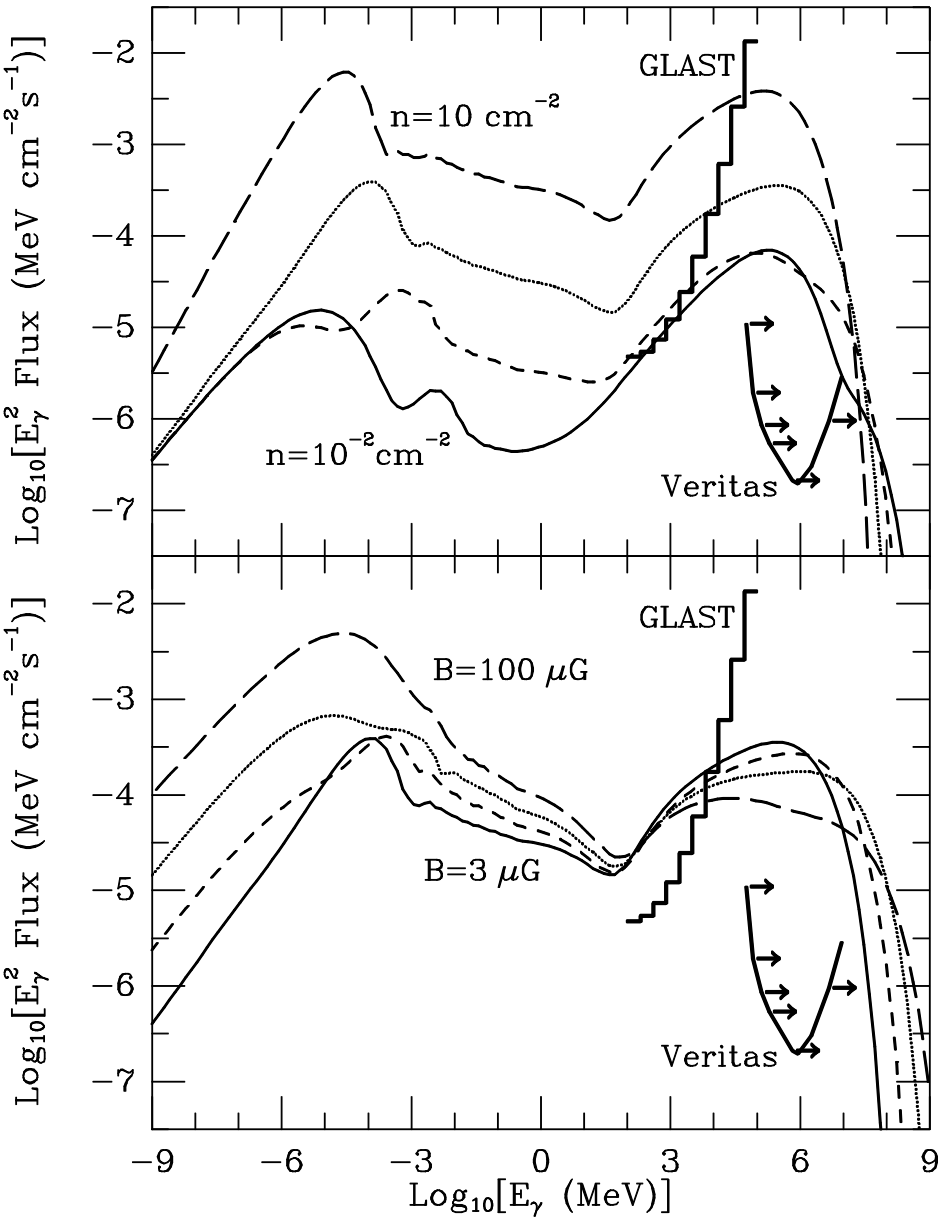

FIGURE 2. Trends of total photon emission for variations of ISM parameters $n \equiv n_{\rm ISM}$ and $B \equiv B_{\rm ISM}$, adapted from the simplified approximate description of non-linear acceleration in [35]. Top panel: the ISM field is fixed at $B = 3\mu$G, and the ambient number density is varied such that: $n = 0.01$ cm^{-3} (solid), $n = 0.1$ cm^{-3} (short dashes), $n = 1$ cm^{-3} (small dots), and $n = 10$ cm^{-3} (long dashes). Bottom panel: B is varied: $B = 3\mu$G (solid), $B = 10\mu$G (short dashes), $B = 30\mu$G (small dots), and $B = 100\mu$G (long dashes), with the density pinned to $n = 1$ cm^{-3}. Here $(e/p)_{\rm rel} = 0.03$; consult [35] for other model parameters. Also depicted are the canonical integral flux sensitivity for Veritas [42] and the differential flux sensitivity for GLAST (Digel, private communication) to facilitate the discussion in the text.

Fig. 2. Naively, one expects that the radio-to-X-ray synchrotron and gamma-ray inverse Compton components should scale linearly with density increases, while the bremsstrahlung and pion decay contributions intuitively should be proportional to $n_{\rm ISM}^2$. However, global spectral properties are complicated by the non-linear acceleration mechanism and the evolution of the SNR. As $n_{\rm ISM}$ rises, the expanding supernova sweeps up its ejecta mass sooner, and therefore decelerates on shorter timescales, thereby reducing both the volume $\mathcal{V}$ of a remnant of given age, and lowering the shock speed and the associated downstream ion temperature $T_{\rm pd}$. Hence, the density increase is partially offset by the "shifting" of the particle distributions to lower energies (due to lower $T_{\rm pd}$) so that the normalization $\mathcal{N}$ of the non-thermal distributions at a given energy is a weakly increasing function of $n_{\rm ISM}$. Clearly $\mathcal{V}$ times this normalization controls the observed flux of the synchrotron and inverse Compton components, while the product of $\mathcal{N}$, the target density $n_{\rm ISM}$ and $\mathcal{V}$ determines the bremsstrahlung and $\pi^0 \rightarrow \gamma\gamma$ emission, with results shown in Fig. 2. Observe that the approximate constancy of the inverse Compton contribution effectively provides a lower bound to the gamma-ray flux in the 1 GeV–1 TeV band, a property that is of significant import in defining experimental goals.

The principal property in Fig. 2 pertaining to variations in $B_{\rm ISM}$ is the anti-correlation between radio and TeV fluxes: the higher the value of $B_{\rm ISM}$, the brighter the radio synchrotron, but the fainter the hard gamma-ray pion emission. This property arises because of the influence of the magnetic field on the shock dynamics and total compression ratio r: the higher the value of $B_{\rm ISM}$, the more the field contributes to the overall pressure, reducing the Alfvénic Mach number and accordingly r, as the flow becomes less compressible. This weakening of the shock steepens the particle distributions and the overall photon spectrum. An immediate offshoot of this behaviour is the premise [35] that radio-selected SNRs may not provide the best targets for TeV observational programs. Case in point: Cas A is a very bright radio source while SN 1006 is not, and the latter was observed first.

Since $n_{\rm ISM}$ and $B_{\rm ISM}$ principally determine the gamma-ray spectral shape, flux normalization and whether or not the gamma-ray signatures indicating the presence of cosmic ray ions are apparent, they are the most salient parameters to current and future ACT programs and the GLAST experiment.

KEY ISSUES AND EXPERIMENTAL POTENTIAL

There are a handful of quickly-identifiable key issues that define goals for future experiments, and these can be broken down into two categories: spatial and spectral. First and foremost, the astronomy community needs to know whether the EGRET band gamma-ray emission is actually shell-related. While the associations of [5] were enticing, subsequent research [39–41] has suggested that perhaps compact objects like pulsars and plerions or concentrated regions of dense molecular material may be responsible for the EGRET unidentified sources. If a connection to the shell is eventually established, it is desirable to know if it is localized only

to portions of the shell. One naturally expects that shock obliquity effects [29] can play an important role in determining the gamma-ray flux in "clean" systems like SN 1006, and that turbulent substructure within the remnant (e.g. Cas A) can complicate the picture dramatically. Such clumping issues impact radio/gamma-ray flux determinations, since the radio-emitting electrons diffuse on shorter length scales and therefore are more prone to trapping. Another contention that needs observational verification is whether or not limb-brightening increases with SNR age? Improvements in the angular resolution of ACTs can resolve these issues and discern variations in gamma-ray luminosities across SNR shells: the typical capability of planned experiments such as HESS, Veritas, MAGIC and CANGAROO-III is of the order of 2–3 arcminutes in the TeV band [42,43].

The principal gamma-ray spectral issue is whether or not there is evidence of cosmic ray *ions* near remnant shocks. The goal in answering this is obviously the detection of $\sim 70\,\mathrm{MeV}$ π^0 bump, the unambiguous signature of cosmic ray ions, and given the GLAST *differential* sensitivity (the measure of capability in performing spectral diagnostics as opposed to detection above a given energy) plotted in Fig. 2, GLAST will be sensitive to remnants with $n_{\rm ISM} \gtrsim 0.1\ \mathrm{cm}^{-3}$. Atmospheric Čerenkov experiments can also make progress on this issue, with the dominant component in the super-TeV band for moderately or highly magnetized remnant environs being that of pion decay emission (see Fig. 1). Such a circumstance may already be realized in the recent marginal detection [17] of Cas A by HEGRA. The most powerful diagnostic the sensitive TeV experiments will provide is the determination of the maximum energy (see Fig. 2) of emission (and therefore also that of cosmic ray ions or electrons), thereby constraining $n_{\rm ISM}$, $B_{\rm ISM}$ and the e/p ratio. Furthermore, the next generation of ACTs should be able to discern the expected anti-correlation between $E_{\rm max}$ and γ-ray flux, and with the help of GLAST, search for spectral concavity, a principal signature of non-linear acceleration theory. In view of the anticipated increase in the number of TeV SNRs, a population classification may be possible, determining whether or not SN1006 and other out-of-the-plane remnants differ intrinsically in their gamma-ray and cosmic ray production from the Cas A-type SNRs. These potential probes augur well for exciting times in the next 5–10 years in the field of TeV gamma-ray astronomy.

Acknowledgments: I thank my collaborators Don Ellison, Steve Reynolds, Isabelle Grenier, Frank Jones and Philippe Goret for many insightful discussions, Seth Digel for providing results of simulations of GLAST spectral capabilities, and Rod Lessard for supplying the Veritas integral flux sensitivity data for Fig. 2.

REFERENCES

1. Higdon, J. C. & Lingenfelter, R. E. *Ap. J. Lett.* **198**, L17 (1975).
2. Chevalier, R. A. *Ap. J.* **213**, 52 (1977).
3. Pollock, A. M. T. *Astron. Astr.* **150**, 339 (1985).
4. Dorfi, E. A. *Astron. Astr.* **251**, 597 (1991).

5. Esposito, J. A., Hunter, S. D., Kanbach, G. & Sreekumar, P. *Ap. J.* **461**, 820 (1996).
6. Drury, L. O'C., Aharonian, F. A., & Völk, H. J. *Astron. Astr.* **287**, 959 (1994).
7. Lessard, R. W., et al. *Proc. 24th ICRC (Rome)* **2**, 475 (1995).
8. Prosch, C., et al. *Astron. Astr.* **314**, 275 (1996).
9. Buckley, J. H. et al. *Astron. Astr.* **329**, 639 (1997).
10. Mastichiadis, A., & de Jager, O. C. *Astron. Astr.* **311**, L5 (1996).
11. Baring, M. G. 1997, in *Very High Energy Phenomena in the Universe*, ed. Trân Thanh Vân, J., et al. (Éditions Frontières, Paris), p. 97 & p. 107.
12. Sturner, S. J., Skibo, J. G., Dermer, C. D., & Mattox, J. R. *Ap. J.* **490**, 619 (1997).
13. Baring, M. G., Ellison, D. C., Reynolds, S. P., Grenier, I. A., & Goret, P. *Ap. J.* **513**, 311 (1999).
14. Tanimori, T., et al. *Ap. J. Lett.* **497**, L25 (1998).
15. Pohl, M. *Astron. Astr.* **307**, L57 (1996).
16. Koyama, K. et al. *Nature* **378**, 255 (1995).
17. Völk, H. J., et al. (1999, these proceedings).
18. de Jager, O. C. & Baring, M. G. *Proc. 4th Compton Symposium*, ed. Dermer, C. D. & Kurfess, J. D. (AIP Conf. Proc. 410, New York), p. 171 (1997).
19. Völk, H. J. in *Towards a Major Atmospheric Čerenkov Detector*, ed. O. C. de Jager (Wesprint, Pochefstroom) p. 87 (1998).
20. Drury, L. O'C., Markiewicz, W. J. & Völk, H. J. *Astron. Astr.* **225**, 179 (1989).
21. Eichler, D. *Ap. J.* **277**, 429 (1984).
22. Ellison, D. C., & Eichler, D. *Ap. J.* **286**, 691 (1984).
23. Jones, F. C. & Ellison, D. C. *Space Sci. Rev.* **58**, 259 (1991).
24. Gaisser, T. K., Protheroe, R. J., & Stanev, T. *Ap. J.* **492**, 219 (1998).
25. Reynolds, S. P. *Ap. J. Lett.* **459**, L13 (1996).
26. de Jager, O. C., & Mastichiadis, A. *Ap. J.* **482**, 874 (1997).
27. Berezhko, E. G., & Völk, H. J. *Astroparticle Phys.* **7**, 183 (1997).
28. Berezhko, E. G., Yelshin, V., & Ksenofontov, L. *Sov. Phys. JETP* **82**, 1 (1996).
29. Ellison, D. C., Baring, M. G. & Jones, F. C. *Ap. J.* **473**, 1029 (1996).
30. Ellison, D. C., Möbius, E., & Paschmann, G. *Ap. J.* **352**, 376 (1990).
31. Baring, M. G., et al., *Ap. J.* **476**, 889 (1997).
32. Berezhko, E. G., Ksenofontov, L., & Petukhov, S. I. *Proc. 26th ICRC (Salt Lake City)*, **4**, 431 (1999).
33. Ellison, D. C. & Berezhko, E. G. *Proc. 26th ICRC (Salt Lake City)*, **4**, 446 (1999).
34. Berezhko, E. G. & Ellison, D. C. *Ap. J.* in press (1999).
35. Ellison, D. C., Berezhko, E. G. & Baring, M. G. *Ap. J.* submitted (1999).
36. Berezhko, E. G. *Astroparticle Phys.* **5**, 367 (1996).
37. Berezhko, E. G., & Völk, H. J. *Proc. 26th ICRC (Salt Lake City)*, **4**, 377 (1999).
38. Ellison, D. C., et al. *Proc. 26th ICRC (Salt Lake City)*, **3**, 468 (1999).
39. Brazier, K. T. S., et al., *MNRAS* **281**, 1033 (1996).
40. Keohane, J. W., et al., *Ap. J.* **484**, 350 (1997).
41. Brazier, K. T. S., et al., *MNRAS* **295**, 819 (1998).
42. Weekes, T. C., et al., VERITAS proposal (1999).
43. Kohnle, A. et al. *Proc. 26th ICRC (Salt Lake City)*, **5**, 239 (1999).